University of Sistan and Baluchestan

Chemical Process Design

Available online at http://cpd.usb.ac.ir/


# Unsteady-State Performance and Stabilization Time in Square Cascades for Stable Krypton Isotope Separation

Mohammad Mahdi Shadman [1]✉, Fatemeh Mansourzadeh [2], Valiyollah Ghazanfari [3]

[1] Corresponding Author, Nuclear Fuel Cycle Research School, Nuclear Science and Technology Research Institute, Tehran, Iran.
Email: mshademan@aeoi.org.ir
[2] Corresponding author, Nuclear Fuel Cycle Research School, Nuclear Science and Technology Research Institute, Tehran, Iran.
Email: fmansourzadeh@aeoi.org.ir
[3] Reactor and Nuclear Safety Research School, Nuclear Science and Technology Research Institute, Isfahan, Iran.
Email: vghazanfary@aeoi.org.ir



## ARTICLE INFO

***Article type:***
*Research Article*

***Article history:***
*Received: 2026-06-29*
*Received in revised form: 2026-08-10*
*Accepted: 2026-08-18*
*Available online: 2026-08-18*

***Keywords:*** *Krypton isotope separation; Square cascade; Transient behaviour; Cascade stability; Numerical modeling*

## ABSTRACT

The inherently low single-stage separation factor of stable krypton isotopes makes their enrichment through multistage cascades a challenging task, requiring precise optimization of cascade parameters and a thorough understanding of transient behavior. In this work, we numerically investigate the unsteady-state performance of a square cascade for krypton isotope separation, using a multicomponent mass-balance model discretized by the Crank–Nicolson scheme and solved iteratively via a q-method. The study focuses on how two key design variables—the cascade cut ($\theta$) and the unit mass separation factor ($\alpha$)—affect the stabilization time of individual isotopes and of the entire system. The novelty of this study lies in distinguishing and comparing the stabilization time of individual isotopes with the overall cascade stabilization time, providing a more accurate estimation of the required operating period and avoiding unnecessary operational costs. Simulations are conducted for $\theta$= 0.142 (targeting light isotopes in the product) and $\theta$=0.827 (targeting heavy isotopes in the waste), at $\alpha$ = 1.2 and 1.4. Results reveal that the isotope governing the overall transient response is not fixed: at low cut, intermediate isotope Kr-82 controls the stabilization (184 min), whereas at high cut, the heaviest isotope Kr-86 becomes the rate-limiting component (≈150–884 min depending on α). Increasing α from 1.2 to 1.4 substantially prolongs the global steady-state attainment—from 190 to 481 min at $\theta$=0.142, and from 156 to 941 min at $\theta$=0.827—due to sharper concentration gradients and stronger interstage coupling. These findings demonstrate that steady-state analysis alone is insufficient for cascade design; transient simulation is essential to correctly identify the bottleneck isotope and to optimize start-up strategies. The results provide practical criteria for the design and operation of square cascades.

**Cite this article:** Shadman, M.M., Mansourzadeh, F., Ghazanfari, V., (2026), Unsteady State Performance and Stabilization Time in Square Cascades for Stable Krypton Isotope Separation, *Chemical Process Design*, 5(2), 00-00. http//doi.org/10.22111/cpd.2026.56009.1094


Publisher: University of Sistan and Baluchestan.
DOI: http//doi.org/10.22111/cpd.2026.56009.1094

## 1. Introduction

Stable isotopes (e.g., $^{2}H$, $^{13}C$, $^{15}N$, $^{18}O$) have become indispensable tracers in both medicine and industry, because they enable quantitative pathway and source attribution without the radiological burdens of radioisotopes. In clinical and translational research, stable isotope-resolved metabolomics (SIRM) and in vivo $^{13}C/^{15}N$ tracing are now routinely used to reconstruct metabolic fluxes in complex systems (notably cancer), link genotype to phenotype, and interrogate drug mechanism and resistance—capabilities that have expanded rapidly with high-resolution MS/NMR workflows and improved computational inference of isotopologue patterns [1, 2]. In routine diagnostics, $^{13}C$ breath tests (e.g., for Helicobacter pylori) provide accurate, non-invasive functional readouts and are supported by modern clinical guidance [3, 4]. In human physiology and nutrition, the doubly labeled water method remains a reference approach for measuring free-living total energy expenditure, with recent large-dataset work refining calculation methodology and uncertainty sources [5]. Beyond healthcare, stable isotopes underpin industrial and regulatory applications such as forensics and authenticity (e.g., compound-specific isotope analysis to verify origin or adulteration of foods and bio-products), as well as process tracing in complex supply chains-progress driven by advances in isotope-ratio instrumentation and compound-specific methods that improve sensitivity and discrimination power [6].

In addition to these widely applied isotopes, noble gas isotopes have emerged as highly informative tracers in environmental and geochemical studies. Stable isotopes of krypton (notably Kr-82, Kr-83, Kr-84, and Kr-86) have emerged as powerful tracers in environmental, hydrogeological, and geochemical studies due to their chemical inertness and sensitivity to purely physical fractionation processes. Variations in krypton isotope ratios (e.g., Kr-86/Kr-84 and Kr-83/Kr-84) have been shown to record mass-dependent fractionation associated with gas diffusion, phase exchange, and subsurface transport, enabling detailed investigation of gas migration and recharge processes in deep vadose zones [7]. Experimental and modeling studies further demonstrate that molecular diffusion of krypton in water induces negligible isotopic fractionation, supporting the use of stable krypton isotopes as conservative tracers in aquatic and groundwater systems [8]. Recent methodological advances, including large-volume equilibration techniques coupled with high-precision mass spectrometry, have significantly improved the analytical resolution of dissolved noble gas stable isotope measurements, thereby expanding their application in hydrological and paleoclimate reconstructions [9]. Beyond Earth surface processes, krypton isotope systematics are also widely applied in mantle geochemistry and planetary science to constrain the origin and evolution of volatile reservoirs, including the identification of chondritic signatures in Earth's mantle and extraterrestrial materials [9].

Alternative methods for the enrichment of stable krypton isotopes exploit cryogenic phase transitions and multistage distillation. In cryogenic freezing and partial condensation, heavier isotopes such as Kr-86 preferentially partition into the condensed or solid phase, producing measurable isotopic fractionation. Controlled multistage cryogenic distillation further enhances separation by leveraging subtle differences in vapor pressures and kinetic effects, providing practical pathways for stable Kr isotope enrichment without high-speed mechanical separation [10].With the factor for single-stage separation being low, multistage or connected separation structures are employed to achieve the desired isotopic enrichment. In the theory and design of multicomponent isotope separation processes, square cascade configurations serve as a fundamental analytical construct due to their uniform stage flow characteristic, which simplifies the mass transfer and balance equations across cascade stages. Such simplification enables detailed numerical modeling of isotope concentration profiles and exploration of design parameters without complex stage-by-stage variability. Moreover, square cascades act as reference structures for comparing alternative cascade designs (e.g., R-cascades or ideal cascades) in terms of separative performance and optimal parameter settings. These

models provide insights into how stage number, cut values, and feed positioning influence overall separation efficiency for stable isotope mixtures, making square cascade analyses valuable in both theoretical development and practical optimization of separation schemes beyond specific separation technologies [11-13].

The main novelty of this work is the separate evaluation of the stabilization time of each isotope and the overall cascade stabilization time. Unlike conventional approaches that generally consider only the global steady-state behavior, this analysis provides insight into the transient response of individual isotopic components. Such information can be practically valuable for optimizing cascade operation by avoiding excessive operating time after stabilization, leading to reduced energy consumption and improved economic efficiency. In this study, a transient square cascade was employed for the separation of krypton isotopes, with the aim of investigating the cascade's stability over time. Furthermore, to highlight the significance of the topic in transient cascades, the effects of the separation factor and cascade cut parameters on the overall stability time of the cascade and its isotopes were examined.

## 2. Modeling framework and numerical solution

The square cascade considered in this study consists of multiple stages, each characterized by specific flow rates and isotope concentrations. In the $n$-th stage, $C_{i,n}$ , $C'_{i,n}$ and $C''_{i,n}$ represent the concentrations of the $i$-th isotope in the feed, light product, and heavy product streams, respectively. The feed, product, and waste streams are denoted by $F$, $P$, and $W$. $G_n$ indicates the input flow to the stage, while $L'_n$ and $L''_n$ are the upstream and downstream flow rates. $H_n$ corresponds to the hold-up of the stage.

$$\frac{\partial\left(H_n\hat{C}_{i,n}\right)}{\partial t}=L'_{n-1}C'_{i,n-1}+L''_{n+1}C''_{i,n+1}-L'_nC'_{i,n}-L''_nC''_{i,n}+C \tag{1}$$

where the concentration parameter ($C$) is defined by

$$C=\begin{cases}FC_{i,F} & n=N_F\\ 0 & n\neq N_F\end{cases} \tag{2}$$

The following algebraic equations are obtained from the discretization using the Crank–Nicolson method and material balance.

$$A_nC'^{m+1}_{i,n-1}+B_nC'^{m+1}_{i,n}+E_nC''^{m+1}_{i,n}+D_nC''^{m+1}_{i,n+1}=R^m_{i,n} \tag{3}$$

where coefficients $A$, $B$, $D$, $E$, and $R$ constitute the system matrix of the resulting algebraic equations. To solve the resulting system of algebraic equations, a q-iteration approach is employed [13].

The q-value is defined as the ratio of the isotope concentration in the product stream to that in the waste stream:

$$q_{i,n}=\frac{C'_{i,n}}{C''_{i,n}} \tag{4}$$

where $C'_{i,n}$ and $C''_{i,n}$ represent the concentrations of isotope i in the product and waste streams of stage n, respectively. For the reference isotope $k$, an initial value of $q_{k,n}$ is assumed, and the $q$-values of other isotopes are calculated using the mass-dependent separation relationship:

$$q_{i,n}=q_{k,n}\alpha^{M_k-M_i} \tag{5}$$

The calculated $q$-values are incorporated into the coupled isotope mass-balance equations, and the isotope concentrations are updated by solving the discretized equations. At each time step, the $q$-values are adjusted iteratively until the isotope concentration normalization condition is satisfied:

$$\sum_i C_{i,n} = \sum_i C'_{i,n} = \sum_i C''_{i,n} = 1 \tag{6}$$

The proposed framework accounts for multicomponent separation through the use of binary separation factors, thereby linking the separation behavior of individual isotopes to the overall performance of the cascade. Through successive iterations, isotope concentrations and flow rates are updated in a manner that simultaneously satisfies mass-balance constraints and separation requirements at all stages. To ensure convergence to a steady-state solution, the following convergence criterion was implemented:

$$\sum_i \left| FC_{i,F} - PC'_{i,N} - WC''_{i,1} \right|^{(t)} < \varepsilon \tag{7}$$

where ε represents the steady-state error, set to 0.0001 in this study. This equation represents the convergence criterion for the $i$-th isotope.

It should be noted that the assumptions of constant stage holdup and the mass-dependent separation factor equation (Eq. (5)) are adopted to simplify the numerical formulation while preserving the essential characteristics of isotope separation behavior.

## 3. Results and discussion

To evaluate the reliability of the developed numerical model, its predictions were validated against the published results reported in [14]. Since no experimental data were available for the present study, validation was performed by comparing the numerical results with a well-established reference model for xenon isotope separation. The validation was carried out for a cascade consisting of 100 stages, with the feed stream introduced at stage 50. The stage flow rate to feed flow rate ratio was set to 10, the cascade cut was 0.85, the unit mass separation parameter was 1.4, and the holdup of each stage was assumed to be 0.3 g, consistent with the conditions reported in [14].

The concentration distributions obtained from [14] and those predicted by the present model are presented in Fig. 1(a) and Fig. 1(b), respectively. As can be observed, the predicted the steady-state error are in good agreement with the published results, confirming the accuracy and reliability of the developed numerical model. Therefore, the proposed model can be confidently employed to investigate the transient behavior and stabilization characteristics of isotope separation cascades.

In a square cascade for isotope enrichment, the structural simplicity stems from maintaining a constant feed flow into each stage and identical stage configuration throughout the cascade, which influences how the separation factor (α) and the cascade cut (θ) govern enrichment performance. The unit separation factor determines the per-stage ability to discriminate between isotopes; when α is close to unity—as is typical for noble gases such as krypton—the overall cascade must compensate with a larger number of stages or optimized cut values to achieve significant isotope enrichment. Because all stages in a square cascade share the same flow and equipment, the choice of cascade cut becomes crucial: it controls the fraction of feed diverted to the product stream versus tails, directly affecting separative work, product assay, and overall throughput. Unlike tapered cascades, square cascades tend to be less efficient due to inherent mixing when equal cuts are applied, but they offer structural uniformity and can be systematically optimized for specific isotope targets by adjusting θ in tandem with α and stage count [12].

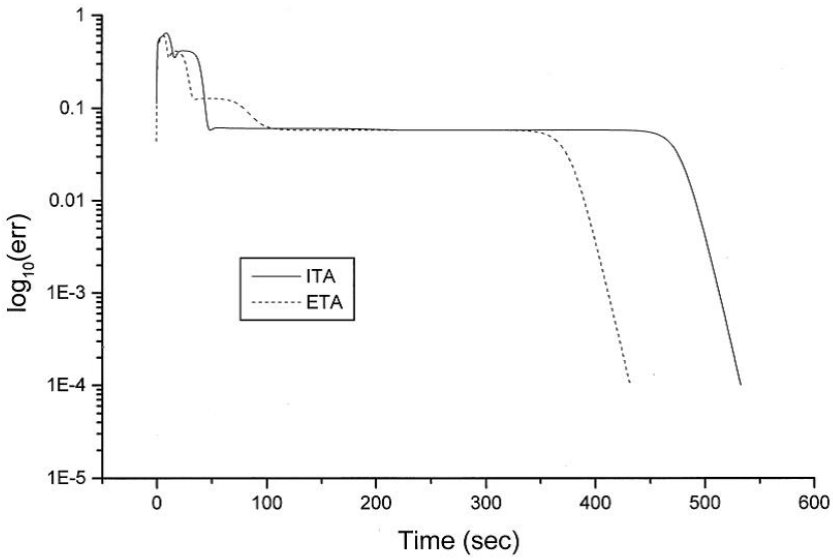


(a)

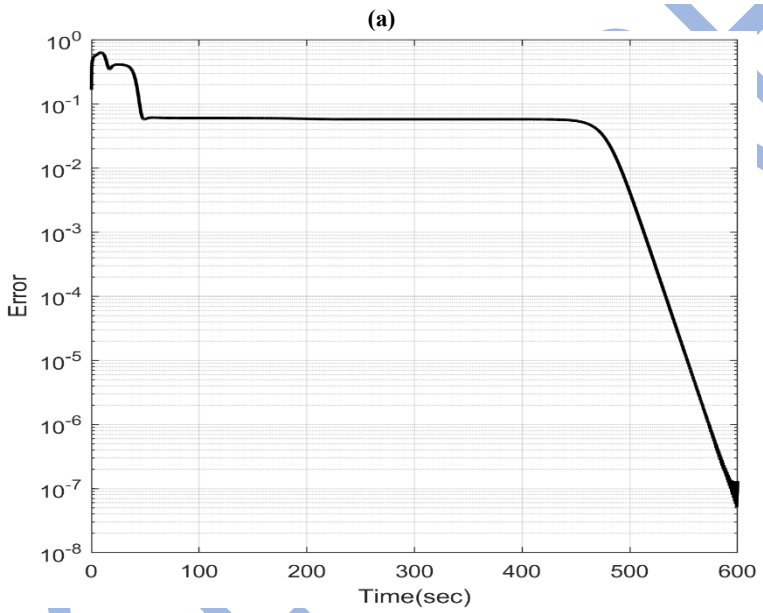


(b)

**Fig. 1**. Comparison between (a) the results of the developed model and (b) the reference results reported in [14]

The characteristics of the square cascade investigated in this study are summarized in Table 1. The cascade consists of a uniform arrangement of identical separation stages, consistent with the definition of a square cascade, in which the number of stages, stage inventory, and feed flow remain constant throughout the system. The natural isotopic composition of krypton used as the cascade feed is given in Table 2. The initial isotopic concentrations in all cascade stages were assumed to be equal to the corresponding isotopic concentrations of the feed stream listed in Table 2. These initial conditions were used to initialize the transient simulation.

**Table 1**. Specifications of the square cascade used in this study

| Feed stage | Number of stages | First-stage cut | Ratio of stage feed to cascade feed | Feed flow rate (gr/min) | Gas inventory per stage (gr) |
|---|---|---|---|---|---|
| 9 | 20 | 0.5 | 5 | 2 | 1 |

**Table 2**. Natural isotopic abundances of krypton

| Isotope | Kr-78 | Kr-80 | Kr-82 | Kr-83 | Kr-84 | Kr-86 |
|---|---|---|---|---|---|---|
| Mole fraction (%) | 0.36 | 2.29 | 11.6 | 11.5 | 57.0 | 17.3 |

In order to investigate the effect of the cascade cut and the separation factor on the time required for a transient square cascade to reach steady state, two cut values, $\theta = 0.142$ and $\theta = 0.827$, are considered for the cascade under study. The first cut value corresponds to the sum of the molar fractions of the first three isotopes in the cascade feed and is therefore selected to examine the separation of lighter krypton isotopes. The second cut value is equal to the sum of the molar fractions of the first five isotopes in the feed and is chosen with the objective of separating heavier krypton isotopes. In addition, two hypothetical unit separation factors, $\alpha = 1.2$ and $\alpha = 1.4$, are assumed in order to evaluate how variations in per-stage separation efficiency influence the transient behavior of the square cascade and its steady-state establishment time.

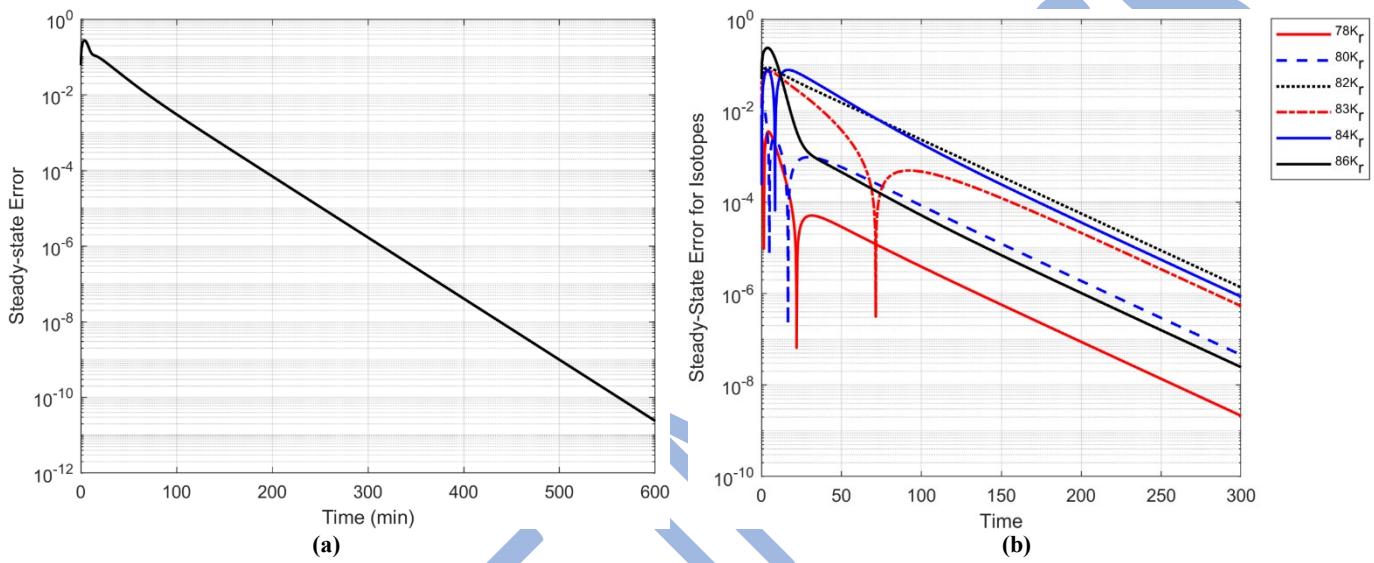


**Fig. 2**. Steady-state error for (a) the entire cascade and (b) each individual isotope ($\theta = 0.142$, $\alpha = 1.2$)

In Fig. 2(a), the steady-state convergence error for the entire cascade and, in Fig. 2(b), the convergence error for individual isotopes are presented. It is observed that the cascade as a whole reaches a steady state—defined here by an error criterion of less than $1\times10^{-4}$—at approximately 190 minutes of operation when $\theta = 0.142$ and $\alpha = 1.2$. In contrast, the lightest isotope attains its steady concentration in less than 2 minutes, indicating that individual isotopic components can equilibrate much faster than the cascade's integrated response. This phenomenon is consistent with transient dynamic simulations reported in the literature, where the redistribution of multi-component isotopic concentrations follows coupled mass balance and separation equations until a global steady state is achieved, with convergence difficulty increasing as the number of components and stages grows. Such modeling approaches underscore that overall cascade stability is governed not only by local isotope behavior but also by cumulative interstage flows and separation dynamics that evolve over time [13].

The observed variation in isotope-specific transient behavior cannot be readily correlated with either the isotopic molar mass or its initial feed concentration, but rather arises from the interplay between mass transport rates and differential separative flows within the cascade. Notably, Isotope-82 acts as the time constant controlling the approach to steady state for the full cascade, likely because intermediate isotopes with moderate abundance and separation factor sensitivity require extended redistribution across the stages before equilibrium is reached. Comparable conclusions have been drawn in studies of transient square cascades, where different isotopes reach optimal separation at distinct times depending on system parameters, and where the cut and unit separation factor significantly influences the time required for the cascade to stabilize. Fig. 3 illustrates the transient evolution of isotopic concentrations in the

cascade withdrawals as a function of time for a square cascade operating with a cut of $\theta = 0.142$ and a unit separation factor of $\alpha = 1.2$. Fig. 3(a) presents the concentration profiles in the product withdrawal, while Fig. 3(b) shows the corresponding behavior in the waste withdrawal.

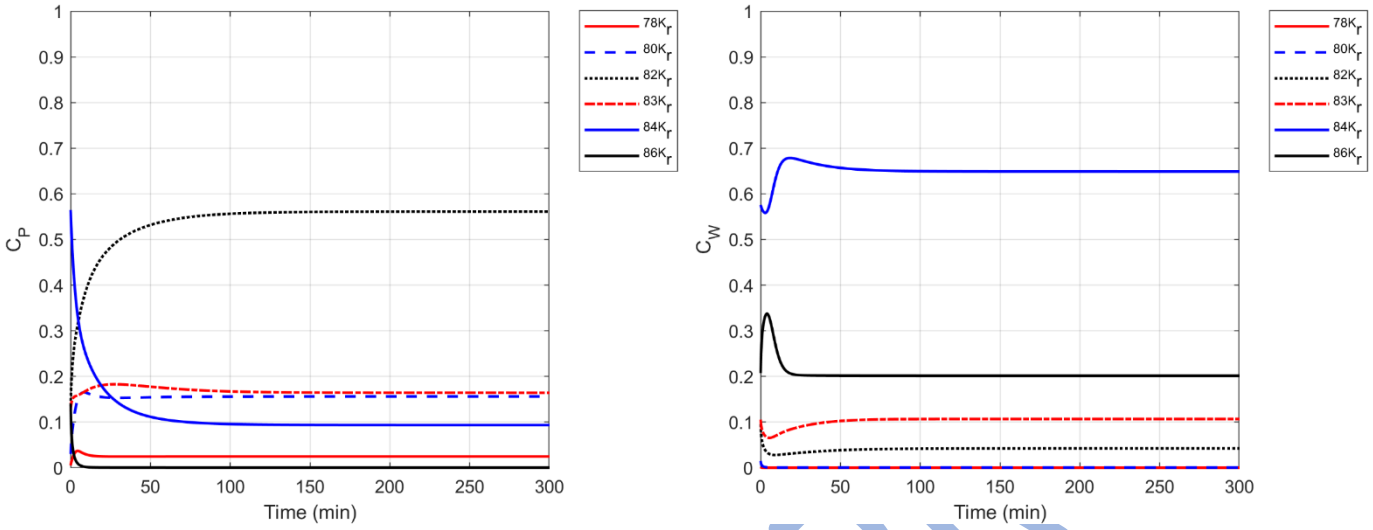


**(a)** **(b)**

**Fig. 3**. Isotopic concentration in the cascade withdrawals as a function of time: (a) in the product, (b) in the waste ($\theta = 0.142$, $\alpha = 1.2$)

As observed in Fig. 3(a), lighter and intermediate krypton isotopes exhibit markedly different transient responses in the product stream. In particular, Kr-82 shows a gradual monotonic increase and ultimately dominates the product composition at steady state, whereas Kr-84 initially appears at relatively high concentration and then decreases as the cascade approaches equilibrium. This overshoot behavior reflects the transient redistribution of isotopes along the cascade stages, which is characteristic of square cascades where identical stage inventories and uniform flows lead to delayed global equilibration. Lighter isotopes such as Kr-78 rapidly decay to very low concentrations in the product stream, consistent with the low cut value favoring the withdrawal of lighter components and the limited per-stage separation capability associated with $\alpha = 1.2$. Fig. 3(b) demonstrates the complementary behavior in the waste withdrawals. Heavier isotopes, particularly Kr-84 and Kr-86, rapidly accumulate in the waste stream and reach their steady-state concentrations within relatively short times compared to the overall cascade stabilization time. Intermediate isotopes such as Kr-82 and Kr-83 exhibit slower convergence and mild transient extrema, indicating that their redistribution between product and waste streams governs the long-term dynamic response of the cascade. This observation is consistent with earlier findings that intermediate isotopes often control the characteristic time constant of transient square cascades, as their separation is most sensitive to both the cascade cut and the separation factor [13]. Consequently, although individual isotopes may stabilize quickly in one withdrawal stream, the coupled mass balances across all stages delay the attainment of a fully steady isotopic distribution throughout the cascade.

Fig. 4a (t = 10 min) and Fig. 4b (t = 20 min), present the distribution of krypton isotope concentrations in the product stream of the square cascade as a function of stage number. A comparison of these two figures shows that the overall trends of the isotopic concentration profiles along the cascade stages are similar at both times; however, the degree of separation and the level of isotopic enrichment change with time, reflecting the transient nature of the process. In both figures, heavier isotopes such as Kr-84 and Kr-86 exhibit higher concentrations at the lower-numbered stages

and gradually decrease toward the higher stages, whereas lighter isotopes, including Kr-78 and Kr-80, display the opposite behavior, with their concentrations increasing along the cascade.

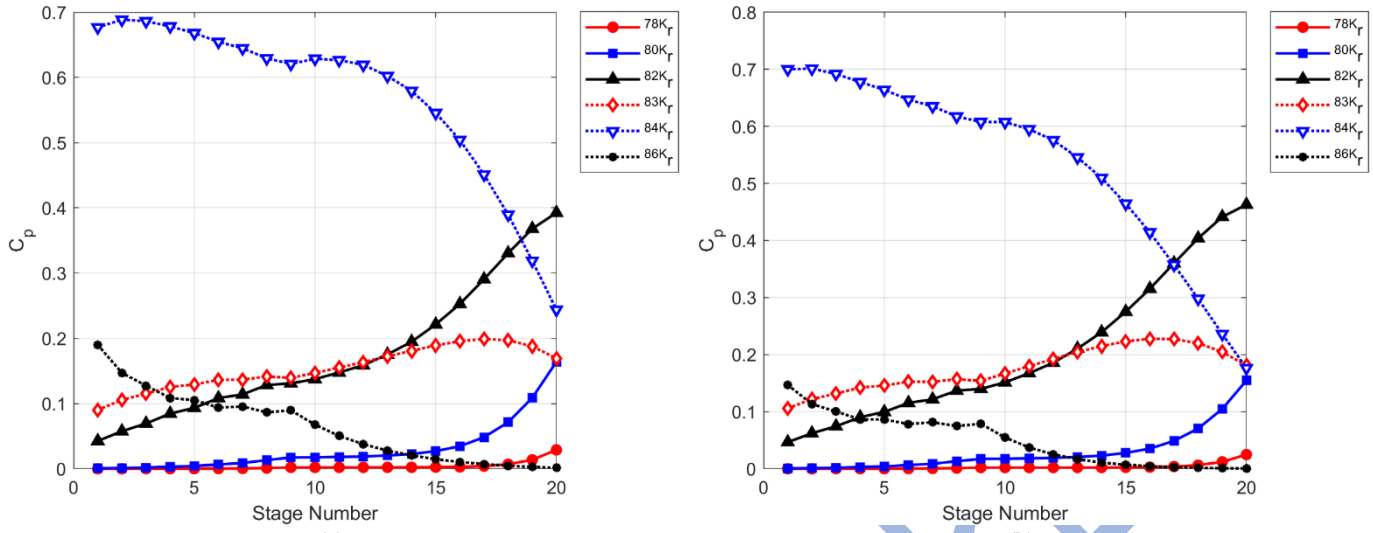


**Fig. 4**. Transient isotopic concentration profiles in the product stream of the square cascade as a function of stage number at (a) $t$ = 10 min and (b) $t$ = 20 min ($\theta$ = 0.142, $\alpha$ = 1.2)

This consistent pattern indicates that the separation mechanism is established early in the operation. Nevertheless, as time progresses from 10 minutes to 20 minutes, the magnitude of concentration differences between isotopes increases, and the separation becomes more pronounced, demonstrating the gradual strengthening of isotopic separation as the cascade evolves toward steady state. Intermediate isotopes, particularly Kr-82 and Kr-83, show similar profile shapes at both times but with noticeable changes in concentration levels along the stages. This observation suggests that while the relative ordering of isotope distributions remains largely unchanged during the early transient period, the intensity of separation and enrichment continuously evolves with time. Consequently, these results highlight the importance of transient analysis in square cascades, as time-dependent effects play a crucial role in determining the extent of isotope separation, which cannot be fully captured by steady-state analysis alone.Table 3 summarizes the time required for each isotope and the entire cascade to reach a steady state under four different combinations of cascade cut (θ) and separation factor (α). The analysis of these data reveals that the stabilization time of the cascade and the controlling isotope are strongly dependent on both the cascade cut and the separation factor. At low cut values (θ = 0.142), the separation target was the lighter isotopes (Kr-78 to Kr-82) in the product stream. In this scenario, the third isotope (Kr-82) exhibits the longest time to reach steady state, thereby acting as the controlling isotope for the overall cascade stabilization. Conversely, at high cut values (θ = 0.827), the separation focus shifts to the heavier isotope (Kr-86) in the waste stream, and the final isotope (Kr-86) demonstrates the longest stabilization time, serving as the controlling isotope.

**Table 3**. Steady-state time of each isotope and the entire cascade as a function of separation factor and cascade cut

| Separation factor | Cut | Kr-78 | Kr-80 | Kr-82 | Kr-83 | Kr-84 | Kr-86 | Cascade |
|---|---|---|---|---|---|---|---|---|
| 1.2 | 0.142 | 1.5 | 4.9 | 184.5 | 70 | 8.5 | 84.4 | 190.4 |
| 1.4 | 0.142 | 0.6 | 1.3 | 463.5 | 55.5 | 368.7 | 94.7 | 481.1 |
| 1.2 | 0.827 | 8.5 | 18.8 | 74.7 | 92.2 | 12.5 | 149.8 | 156.1 |
| 1.4 | 0.827 | 5.9 | 10.6 | 125.4 | 317.4 | 0.01 | 884.3 | 940.6 |

These results indicate that the controlling isotope is determined by the selected cascade cut and depends on whether the separation goal prioritizes light isotopes in the product or heavy isotopes in the waste. The effect of the separation factor is also significant. Increasing α from 1.2 to 1.4 substantially extends the time required for certain isotopes and the entire cascade to reach steady state. For example, at $\theta$ = 0.142, the stabilization time of Kr-82 increases from 184.5 minutes to 463.5 minutes, while the total cascade stabilization time rises from 190.4 minutes to 481.1 minutes. From a transport perspective, a higher unit separation factor increases the isotopic discrimination at each stage, which results in stronger enrichment and depletion zones along the cascade. Although this improves the separation capability of individual stages, it also generates steeper concentration gradients between adjacent stages.

During transient operation, these gradients must be redistributed through the interstage flows before the entire cascade can achieve equilibrium. Therefore, the stronger stage-wise separation associated with higher α values increases the time required for the coupled multicomponent system to relax toward its steady-state distribution. In other words, a higher separation factor enhances the final separation performance but can slow down the transient approach to equilibrium because the cascade requires a longer period to establish the new concentration profile throughout all stages. It should be noted that the very short stabilization time obtained for Kr-84 at $\alpha$ = 1.4 and $\theta$ = 0.827 corresponds to the rapid convergence of its withdrawal concentration according to the isotope-specific criterion. This value does not represent the stabilization time of the entire cascade, which is controlled by the slowest transient mode of the coupled multicomponent system.

In summary, the selection of the cascade cut not only determines the separation target but also identifies the controlling isotope for cascade stabilization. Furthermore, increasing the separation factor, while improving stage-wise separation efficiency, leads to slower transient dynamics and longer times to reach steady state. These findings provide practical guidance for the design and optimization of square cascades in isotope separation, particularly for noble gases.

Beyond these parameter-specific trends, the broader context of transient cascade research and the practical implications of the identified rate-limiting behavior warrant further discussion. Previous transient studies on square cascades have largely concentrated on steady-state parameter optimization or on identifying the time at which each isotope reaches its peak enrichment. However, the fundamental question of which specific isotope governs the overall stabilization time of the entire cascade, and how this role shifts with operating conditions, has received less systematic attention. In some earlier simulations for other noble gases, the heaviest isotope was observed to exhibit the longest equilibration time, yet this finding was not generalized as a universal rule across different cut ratios and separation factors.

The present results fill this gap by clearly demonstrating that the rate-limiting isotope is not an intrinsic, fixed property of the element, but rather a function of the cascade design objective; it shifts from an intermediate-mass isotope (at low cut) to the heaviest isotope (at high cut). This condition-dependent behavior has not been directly identified in previous transient analyses, where most studies assumed a fixed controlling isotope over the entire parameter range—an assumption that can lead to inaccurate predictions of start-up duration. From a practical engineering standpoint, these findings directly inform the design of monitoring systems, start-up scheduling, and economic assessments: first, by enabling a focused monitoring strategy that tracks only the bottleneck isotope—predictably determined by the selected cut—rather than all isotopes simultaneously, thereby reducing control complexity and instrumentation costs; second, by providing quantitative criteria for optimal start-up scheduling that avoid both premature product

withdrawal (which would compromise purity) and unnecessarily prolonged operation (which wastes energy and feed); and third, by highlighting a critical economic trade-off—namely, that increasing the unit separation factor ($\alpha$) to improve per-stage resolution comes at the cost of substantially longer transient periods, especially at high cut ratios, so that a slightly lower α may sometimes yield a lower total process cost by significantly shortening the equilibration time, even if the steady-state enrichment is marginally reduced. This last consideration is particularly important for noble gas systems with separation factors close to unity, which inherently require many stages and long equilibration times to achieve appreciable enrichment.

The present study is based on several simplifying assumptions. The square cascade is considered as an idealized configuration with identical stages, constant stage holdup, and uniform flow characteristics. In addition, the unit separation factor is assumed to be constant and determined according to the mass-dependent separation relationship between isotope pairs. These assumptions allow the fundamental transient behavior of the cascade to be investigated; however, real separation systems may exhibit variations in separation efficiency due to operating conditions and hydrodynamic effects. Furthermore, the present analysis considers a limited range of cascade cuts and separation factors to clarify the effect of key parameters on stabilization behavior. Future studies should extend this framework by considering variable stage holdup, experimentally determined separation factors, and broader operating conditions.

## 4. Conclusions

This study investigates the transient behavior of a square cascade for stable krypton isotope separation using a numerical multicomponent modeling framework. The results demonstrate that cascade stabilization is governed by time-dependent multicomponent interactions rather than by the dynamics of individual isotopes. The time to reach steady state is highly sensitive to both the cascade cut and the unit separation factor. The isotope controlling the overall stabilization time depends on the separation objective: at low cut values targeting lighter isotopes in the product stream, intermediate isotopes such as Kr-82 dominate the transient response, whereas at higher cut values aimed at heavier isotopes in the waste stream, Kr-86 becomes the limiting component. Moreover, increasing the unit separation factor, while improving stage-wise separation efficiency, significantly prolongs the overall stabilization time due to stronger interstage coupling and slower dynamic modes. These findings highlight the necessity of incorporating transient analyses into the design and optimization of square cascade systems, as steady-state analyses alone may yield incomplete or misleading performance evaluations.

## Nomenclature

### Symbols

| | | | |
|---|---|---|---|
| $C_{i,n}$ | Concentration of isotope $i$ in the feed stream of $n$-th stage | $n$ | Stage number |
| $C'_{i,n}$ | Concentration of isotope $i$ in the product stream of $n$-th stage | $P$ | Product flow rate |
| $C''_{i,n}$ | Concentration of isotope $i$ in the waste stream of $n$-th stage | $q$ | Product-to-waste concentration ratio |
| $F$ | Feed flow rate | $t$ | Time (min) |
| $G_n$ | Feed flow entering stage $n$ | $W$ | Waste flow rate |
| $H_n$ | Stage holdup (g) | **Greek symbols** | |
| $i$ | Isotope index | $\alpha$ | Unit mass separation factor |
| $L'_n$ | Upstream interstage flow rate | $\theta$ | Cascade cut |
| $L''_n$ | Downstream interstage flow rate | $\varepsilon$ | Steady-state convergence criterion (error) |

## References

[1] Bruntz, R.C., Lane, A.N., Higashi, R.M., Fan, T.W.-M., 2017. Exploring cancer metabolism using stable isotope-resolved metabolomics (SIRM), Journal of Biological Chemistry, 292 (28), 11601–11609. https://doi.org/10.1074/jbc.R117.776054

[2] Schmidt, D.R., Patel, R., Kirsch, D.G., Lewis, C.A., Vander Heiden, M.G., Locasale, J.W., 2021. Metabolomics in cancer research and emerging applications in clinical oncology, CA: A Cancer Journal for Clinicians, 71 (4), 333–358. https://doi.org/10.3322/caac.21670

[3] Hammer, H.F., Fox, M.R., Keller, J., Salvatore, S., Basilisco, G., Hammer, J., Lopetuso, L., Benninga, M., Borrelli, O., Dumitrascu, D., Hauser, B., Herszenyi, L., Nakov, R., Pohl, D., Thapar, N., Sonyi, M., European H2-CH4-breath test group, 2022. European guideline on indications, performance, and clinical impact of hydrogen and methane breath tests in adult and pediatric patients: European Association for Gastroenterology, Endoscopy and Nutrition, European Society of Neurogastroenterology and Motility, and European Society for Paediatric Gastroenterology Hepatology and Nutrition consensus, United European Gastroenterology Journal, 10 (1), 15–40. https://doi.org/10.1002/ueg2.12133

[4] Lemos, F.F.B., de Castro, C.T., Luz, M.S., Rocha, G.R., Santos, G.L.C., de Oliveira Silva, L.G., Calmon, M.S., Souza, C.L., Zarpelon-Schutz, A.C., Teixeira, K.N., Queiroz, D.M.M., de Melo, F.F., 2024. Urea breath test for Helicobacter pylori infection in adult dyspeptic patients: A meta-analysis of diagnostic test accuracy, World Journal of Gastroenterology, 30 (6), 579. https://doi.org/10.3748/wjg.v30.i6.579

[5] Speakman, J.R., Yamada, Y., Sagayama, H., Berman, E.S., Ainslie, P.N., Andersen, L.F., et al., 2021. A standard calculation methodology for human doubly labeled water studies, Cell Reports Medicine, 2 (2), 100203. https://doi.org/10.1016/j.xcrm.2021.100203

[6] Liu, H., Nie, J., Liu, Y., Wadood, S.A., Rogers, K.M., Yuan, Y., Gan, R.-Y., 2023. A review of recent compound-specific isotope analysis studies applied to food authentication, Food Chemistry, 415, 135791. https://doi.org/10.1016/j.foodchem.2023.135791

[7] Seltzer, A.M., Severinghaus, J.P., Andraski, B.J., Stonestrom, D.A., 2017. Steady state fractionation of heavy noble gas isotopes in a deep unsaturated zone, Water Resources Research, 53 (4), 2716–2732. https://doi.org/10.1002/2016WR019655

[8] Tyroller, L., Brennwald, M.S., Busemann, H., Maden, C., Baur, H., Kipfer, R., 2018. Negligible fractionation of Kr and Xe isotopes by molecular diffusion in water, Earth and Planetary Science Letters, 492, 73–78. https://doi.org/10.1016/j.epsl.2018.03.047

[9] Ng, J., Tyne, R., Seltzer, A., Noyes, C., McIntosh, J., Severinghaus, J., 2023. A new large-volume equilibration method for high-precision measurements of dissolved noble gas stable isotopes, Rapid Communications in Mass Spectrometry, 37 (7), e9471. https://doi.org/10.1002/rcm.9471

[10] Cholach, A., Yakovin, D., Latkin, N., Sidorov, I., 2023. Freezing-out of heavy isotopes of Kr, arXiv preprint, arXiv:2311.18404. https://doi.org/10.48550/arXiv.2311.18404

[11] Garza Adl, G.A., Garrett, G.A., Murphy, J.E., 1962. Multicomponent isotope separation in cascades, Chemical Engineering Science, 15 (3–4), 188–209. https://doi.org/10.1016/0009-2509(61)85023-9

[12] Khooshechin, S., Mansourzadeh, F., Imani, M., Safdari, J., Mallah, M.H., 2021. Optimization of flexible square cascade for high separation of stable isotopes using enhanced PSO algorithm, Progress in Nuclear Energy, 140, 103922. https://doi.org/10.1016/j.pnucene.2021.103922

[13] Shadman, M.M., Ghazanfari, V., Amini, Y., Mansourzadeh, F., Khamseh, A.G., Khani, M.H., Hassanvand, A., Heydari, M., 2023. Optimal time separation modeling and simulation for stable neon isotopes in a transient square cascade: A comprehensive study, SN Applied Sciences, 5 (12), 361. https://doi.org/10.1007/s42452-023-05589-0

[14] Zeng, S., Ying, C., 2000. A second-order time-accurate method for determination of concentration distribution of multicomponent mixtures in separation cascades, Separation Science and Technology, 35 (5), 729–741. https://doi.org/10.1081/SS-100100187